CrystEngComm

Accepted Manuscript

ROYAL SOCIETY OF CHEMISTRY

www.rsc.org/crystengcomm

Cite this: DOI: 10.1039/c0xx00000x

www.rsc.org/xxxxxx

ARTICLE TYPE

Transition metal inclusion in RhoZMOF material

Guillermo Calleja[a*], Carmen Martos[a], Gisela Orcajo[a], José A. Villajos[a] and Juan A. Botas[a]

Received (in XXX, XXX) Xth XXXXXXXXX 20XX, Accepted Xth XXXXXXXXX 20XX

DOI: 10.1039/b000000x

Porous RhoZMOF is a negatively charged zeolite-like MOF material, susceptible to be post-synthesis modified by ion-exchange process, replacing as-synthesized organic cations for transition metals. This material exhibiting open transition metal sites is a very attractive candidate for industrial applications related to clean energy, like electrochemistry and gas storage. In the present work, partial or total Co^{2+}, Ni^{2+} and Cu^{2+} inclusion has been successfully carried out in RhoZMOF structure by ion-exchange treatment. Particularly, complete exchange of $HDMA^+$ for Co^{2+} could be reached at room temperature after 12 h of contacting time. For Cu^{2+}-exchange, a rapid transformation of RhoZMOF structure to a new Cu-rich, crystalline and practically non-porous phase was observed at room temperature, avoiding its appearance and preserving the desired structure when ion-exchange treatment is carried out at -20°C and 6 hours, reaching a partial ion-exchange degree of 30 %. Moreover, for Ni^{2+} ion-exchange treatment at 25 and 0°C, a covering of an amorphous Ni-rich organometallic phase over the crystals were detected by SEM analysis, preventing its appearance when reducing the amount of $HDMA^+$ in the media by developing the ion-exchange process in two steps: $HDMA^+$ for Na^+ and Na^+ for Ni^{2+}. These results provide a post-synthesis modification route for obtaining porous MOF materials containing open transition metal sites, accessible for redox catalysis and selective gas adsorption.

..

Introduction

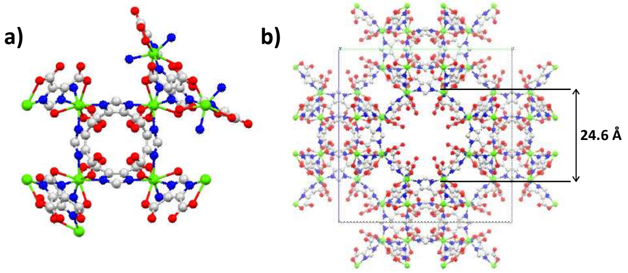

Fig. 1 Detailed coordination of In^{3+} cations to ligands (a) and packed structure (b) of RhoZMOF. Colors: red: oxygen, blue: nitrogen, grey: carbon, and green: indium. Hydrogen atoms were removed for clarity.

Metal-Organic Framework (MOF) materials are fascinating and widely studied solids for many potential applications like molecular separation, chemical sensing, ion-exchange, drug delivery, gas storage and catalysis[1]. They are a new class of porous crystalline materials that can be obtained in high yield by using cheap starting materials, combined with low framework density and high thermal stability, making them interesting candidates for applications related to clean energy technologies. MOFs as gas adsorbents, catalysts and catalyst precursors have been reported for hydrogen storage, CO_2 capture, fuel cells, Li-ion renewable battery and supercapacitors[2,3], being their porosity, proton conductivity and redox properties the most interesting features for these fields.

Among MOF materials, it is possible to identify some zeolite-like structures that exhibit similar topologies to crystalline inorganic microporous zeolite materials but with an expanded network, thus increasing their textural properties like pore size, pore volume and specific surface area. In this kind of materials, the structure is driven by the Metal-Imidazol-Metal bonds which angle is 145°, similar to Si-O-Si angle found in zeolites[4], conferring robustness to the framework. Some of them, as ZIFs (Zeolitic Imidazolate Frameworks), are imidazole-derivative MOFs with neutral structure, commonly composed by divalent metal cations, mainly Zn and Co[5]. Similar imidazole-derivative MOF are found, called, ZMOFs (Zeolite-like Metal Organic Framework) materials, which are built by employing trivalent indium or divalent zinc cations linked by chelating 4,5-imidazoledicarboxylic acid (ImDC) as ligand, yielding negatively charged frameworks that grow around positively charged structure-directing agents (SDA) as imidazonium, dimethyl ammonium ($HDMA^+$), 1,3,4,6,7,8-hexahydro-2H-pyrimido[1,2-a]pyrimidine (HPP^{2+}), 1,2-diaminocyclohexane or guanadinium cations[6-9]. These ZMOF materials are particularly interesting due to their relatively high porosity, hydrothermal stability and especially charged framework[9] subjected to be ion-exchanged for functionalization purposes with organic[6] or metallic cations[8,10-12]. Among them, the most studied is RhoZMOF ($In_{48}(C_5N_2O_4H_2)_{96}(C_2NH_8)_{48}$). This material exhibits RHO zeolitic topology where In is octa-coordinated to 4 N and 4 O atoms, as it is shown in Fig. 1. Depending on the synthesis method, the as-synthesized structure is charge-compensated with HPP^{+2} or $HDMA^+$ organic cations, which can be exchanged by any functionalizing positive-charged species providing accessible active sites for any particular adsorbate/substrate.

In particular, transition metals are potentially useful for gas adsorption and catalysis. In the case of hydrogen adsorption, the increase of the interaction energy between H_2 and this kind of metals has been explained by electrostatic interactions[13] or the possible presence of *Kubas effect*[14]. The inclusion of transition metal cations in catalysts is generally interesting because of the increase of redox and Lewis acid sites, compared to zeolites[15]. Particularly, some examples of transition-metal catalytic properties in energy fields are: as negative electrode in Li-ion batteries[16], as cathode for oxygen reduction reaction in fuel cells and metal-air batteries[17], proton-conductive membranes[18], supercapacitors[16], selective catalytic reduction of NO with ammonia or propane[19], catalytic oxidation of pyridine[20], dehydrogenation and dehydrocyclization of alkenes[21], ethylene production by steam reforming of ethanol[22], and CH_4 reforming[23].

So, the combination of the robustness of a porous zeolite-like MOF structure having imidazole-derivatives in the organic linker and the presence of accessible transition metal ions, constitute a key feature that can promote the activity in redox and acid catalysis, as well as in gas storage.

In our previous works[10,12] alkaline and alkaline-earth ion-exchange post-synthesis treatment have been developed for RhoZMOF material. Herein, we report the ion-exchange modification of RhoZMOF material with transition metals cations like Co^{2+}, Ni^{2+} and Cu^{2+} in order to study kinetics, ion-exchange extension and structure stability after cation inclusion process, in order to provide materials with potential applications in energy storage fields.

Experimental

Materials and Methods

RhoZMOF material was prepared by following the procedure published elsewhere[8] and scaling it up according to the procedure developed by our group[10]. Ion exchange treatment of RhoZMOF material with transition metal ions (Me) was carried out as follows: crystals previously washed with ethanol/water mixture (75 vol. % ethanol) were suspended in the corresponding metallic nitrate solution (0.5 M) in ethanol/water mixture with a Me:In ratio of 33:1 at -20–25°C during 1–72 h. Then, crystals were washed with the same solvent mixture seven consecutive times in order to remove all the remaining non-compensating cations, and were finally submerged in acetonitrile during 3 days, replenishing for fresh solvent three times. Obtained materials were named Me-Rho_T_t, where *Me* refers to the exchanged metallic cation, *T* is temperature in ºC and *t* is time in hours or days.

Characterization Techniques

Powder X-ray diffraction (PXRD) patterns were obtained on a Philips XPERT PRO using CuKα (λ = 1.542 Å) radiation. Scanning electronic microscopy (SEM) images and micro-elemental analysis (EDS) were obtained on a PHILLIPS XL30 ESEM operated at 200 kV. N_2 adsorption isotherms were measured at 77 K on an AutoSorb equipment (Quantachrome Instruments), evacuating the samples under high vacuum for 18 hours, either at 90°C (RhoZMOF) or at 40°C (ion-exchanged RhoZMOF). The micropore surface area and pore volume values were calculated by the Brunauer–Emmett–Teller (BET) model and Non-Local Density Functional Theory (NL-DFT), considering a Kernel model of cylindrical–sphere pores of silica at 77 K. The metal content of the samples was determined by inductively coupled plasma atomic emission spectroscopy (ICP-AES) using a Varian Vista AX CD System Analyzer. For this purpose, 1 mg of the dried MOF material was dissolved in 5 ml of 65 % nitric acid and diluted in 25 ml of water.

Results and discussion

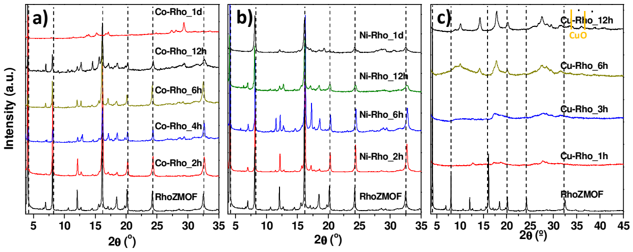

Fig. 2 PXRD of a) Co^{2+}-exchanged, b) Ni^{2+}-exchanged, and c) Cu^{2+}-exchanged RhoZMOF materials at 25°C for different ion-exchange times. Gray dotted lines mark the position of diffraction signals of the simulated PXRD pattern from RhoZMOF-structure single-crystal resolution[6].

The effect of the inclusion of different transition metal ions into RhoZMOF material has been studied over its final structural characteristics. RhoZMOF material was ion-exchanged with divalent cobalt, nickel and copper cations, following the procedure described in the experimental section. Treatment time was the first variable studied, varying from 1 hour to 3 days, depending on each cation. The evolution of crystalline phase was followed by PXRD analysis. Fig. 2-a shows X-ray diffraction patterns for Co^{2+}-exchanged materials, where the characteristic reflections of RhoZMOF are detected up to 12 h. Above this time, a decrease in crystallinity is detected, probably related to the structure degradation. A similar trend was showed for Ni ion-exchanged materials (Fig. 2-b), remaining the principal signals of RhoZMOF phase until to 2 days of treatment. In the case of Cu-exchange process in RhoZMOF material, the behavior changes completely from those for cobalt or nickel, as it is shown in Fig. 2-c. After one hour, an abrupt loss of the structure is detected. After 6 h of treatment, the appearance of a new second phase with low crystallinity was also detected. These new PXRD reflections do not match with those corresponding to copper oxide, discarding the formation of this inorganic specie. In order to confirm the transformation of RhoZMOF to a different crystalline phase, PXRD patterns of the second phase has been refined using X´Pert High Score/Treor90 software. The results shows a possible new phase with tetragonal symmetry $a = b = 13.99$ Å and $c = 19.93$ Å, different from RhoZMOF structure, whose crystal system is cubic with $a = b = c = 31.06$ Å.

Ion-exchange extension, depicted in Fig. 3-a, was calculated by the molar ratio between transition metal and indium content (Me/In), measured by means of ICP technique. For Co- and Ni-exchanged materials, the behavior is quite similar. For short contact times (2-6 h), the ion-exchange degree reached is around 50 % (Me/In = 0.25), being this last 100 % after 12 h. So, similar kinetics was found for Co^{2+} and Ni^{2+} ion-exchange at short times of treatment, possibly due to their similar cation size, and thus their diffusivities into the RhoZMOF material. For longer contact times this ratio overcomes stoichiometric values allowed (Me/In = 0.5). This fact suggests that other process like MOF dissolution and/or new phase formation are taking place in the system. For Cu-treated materials, this last behavior is more evident since the Me/In ratio are even higher for short contact time than expected from the stoichiometry. These results match well with those obtained by PXRD, which showed a loss of the crystalline RhoZMOF phase below 24 h for Ni- and Co- and 1 h for Cu-materials.

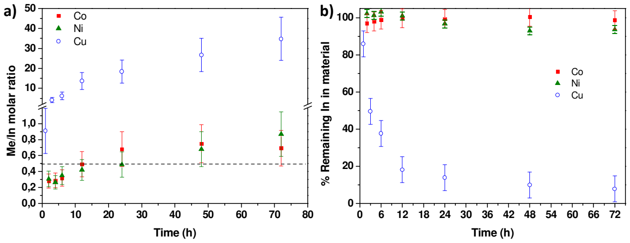

Fig. 3 Evolution of Me/In ratio in RhoZMOF materials after transition-metal ion-exchange (a) and indium content in a 100 % base (b).

In order to confirm the integrity of RhoZMOF framework, structural indium lixiviation was also estimated, analyzing the absolute In content in the samples by ICP technique. Fig. 3-b shows that structural In is maintained (100 %) up to three days for Co-exchanged material, and up to 24 h for the Ni-exchanged solid. Otherwise, Cu-exchanged materials show both a fast reduction of In content and a fast increase in copper content, confirming the formation of a new phase that may be formed by a Cu-rich complex. The new phase, detected previously by PXRD technique, can come from the chemical reaction between transition metals and the negatively charged electron-donor oxygen atoms on dicarboxylic groups from the ligand[6] or the HDMA$^+$ compensating cations. This could be related to the Jahn-Teller distortion effect that shows the coordination sphere of Cu^{2+} [24], that could make the metal more accessible to react with other species in the media, and finally breaking down the ligand-to-Indium bonds in RhoZMOF structure. A similar effect, but in less extension, was observed for Ni-exchanged samples, where a slight decrease of In content was observed for contact times above 24h.

Fig. 4 depicts SEM images taken in backscattered electron mode (BSE) in order to study the morphology and composition of some of the MOF materials obtained showing the RhoZMOF phase with the highest ion-exchange degree. Cobalt- and nickel-modified materials after 6 h of treatment showed a polyhedral morphology characteristic of RhoZMOF crystals[10]. However, for almost all crystals of Ni-Rho sample, another phase darker in color is also detected, indicating the presence of lighter elements, probably organic compounds. EDS elemental microanalysis in the covering phase of Ni- modified material confirmed a higher nickel, carbon and nitrogen content and lower oxygen compared to the clean surface (Fig. S2), which agrees with the results obtained from ICP analysis. HDMA$^+$ is the only C, N-containing and O-free species present in the reaction media that could be involved in the formation of this second phase. Thus, a possible organometallic complex may be made up when migration of HDMA$^+$ compensating cations to the surface of the material, reacting with available Ni cations in the solution.

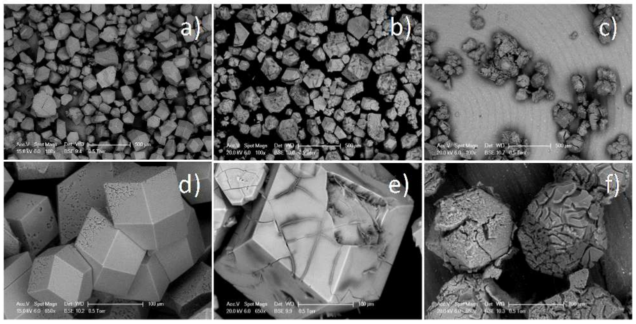

Fig. 4 SEM images collected in the BSE mode after transition metal ion exchange treatment at 25°C for Co 12 h (a,d), Ni 12 h (b,e) and Cu 1 h (c,f).

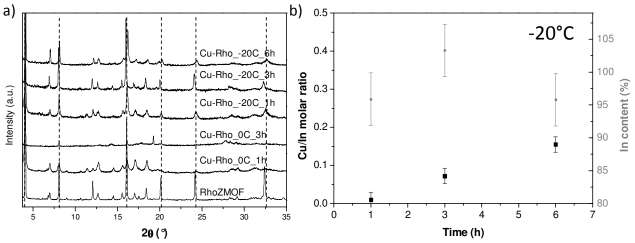

Fig. 5 PXRD (a) and evolution of Cu/In ratio (b) for low temperature Cu-exchanged materials. Gray dotted lines mark the position of diffraction signals of the calculated PXRD pattern from RhoZMOF single-crystal resolution[6].

Finally, copper-exchanged materials show after 1 hour of treatment highly damaged crystals with a residual RhoZMOF-like shape, as a consequence of the phase destruction, previously observed from PXRD and ICP results.

Therefore, complete HDMA$^+$ ion-exchange for Co^{2+} in RhoZMOF structure (Co/In = 0.49) was achieved after 12 h of treatment without a significant loss of the structure. However, extra attempts were needed in order to prevent the formation of the unknown crystalline second phase in Cu treatment and the covering phase in Ni-exchanged material. So, ion–exchange treatment was carried out at lower temperatures (0 and -20°C), trying to decrease the formation rate of the undesired Me-rich phase. Fig. 5-a shows the PXRD patterns for Cu-exchanged materials obtained after treatment at 0°C for 1 and 3 h. For 1 h treatment at 0°C only the RhoZMOF crystal-phase reflections are found. However, after a contact time of 3 hours RhoZMOF structure is lost. For the first case, a very low ion-exchange degree was achieved, only 2.2 % (Cu/In= 0.011 ±0.001, not shown). Nevertheless, when copper treatment is carried out at -20°C, the structure is maintained up to 6 h without the detection of the undesired second crystalline phase. Besides, a reasonable ion-exchange extension of 31 % (Cu/In= 0.154 ± 0.02) is reached, as it is shown in Fig. 5-b. So, for Cu cation inclusion in RhoZMOF framework, ion-exchange process should be accomplished at low temperatures since in these conditions the kinetic of the undesirable phase is slowed down.

On the other hand, Fig. 6-a shows the PXRD patterns for Ni-exchanged materials after treatment at 0°C and different contact times showing the characteristic peaks of RhoZMOF phase up to 6 h and an important reduction of their intensity up to 24 h. Regarding SEM analysis (Fig. 6-b) for the sample prepared at 6 h, the second phase is again detected suggesting it is not crystalline or it is just below the detection limit of the PXRD technique.

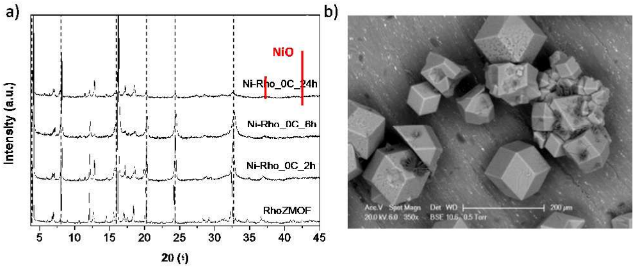

Fig. 6 PXRD (a) and SEM image (b) for 0°C Ni-exchanged materials. Gray dotted lines mark the position of diffraction signals of the calculated PXRD pattern from RhoZMOF single-crystal resolution[6].

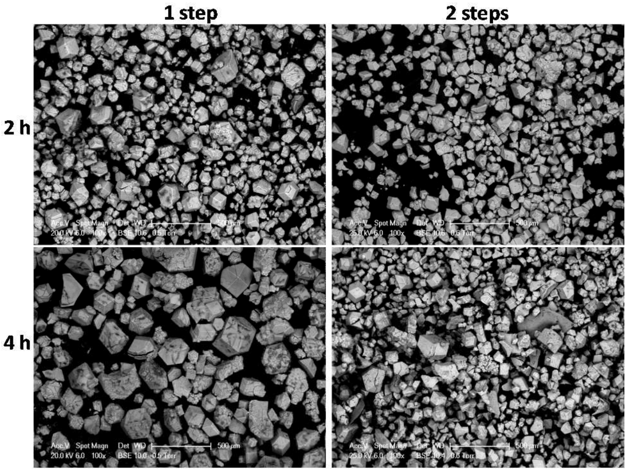

Fig. 7 SEM images for Ni-exchanged RhoZMOF materials obtained in 1 step (left) and 2 steps (right), at 25ºC and different exchanging times.

Finally, a new strategy consisting of reducing the amount of HDMA$^+$ in the media was carried out. For this purpose, the ion-exchange process was developed in two steps, which consisted of a first exchange of HDMA$^+$ for Na$^+$ cations and a second exchange of Na$^+$ for Ni^{2+}. In this second step, lower concentration of organic cations should be present in the reaction media. In the first ion-exchange with sodium, an average Na$^+$-exchange extension of 86 % was reached, providing materials almost free of HMDA$^+$ for the following nickel exchange process. Fig. 7 shows SEM images of final Ni-exchanged materials at 25ºC obtained in 1 step (left) and 2 steps (right) at 2 and 4 h, showing a clean and homogeneous sample free of the darker covering phase over the crystals when the two-step procedure is carried out. The highest ion-exchange extension reached for the sample free of impurities was 22 ± 2 % (molar Ni/In ratio of 0.11±0.09) after 4 h treatment. RhoZMOF phase was also confirmed by PXRD in the two-step exchanged materials (not shown), showing the principal peaks of the desired structure. So, for Ni inclusion in RhoZMOF material, a two-step methodology is proposed in order to avoid the formation of undesired Ni-complexes.

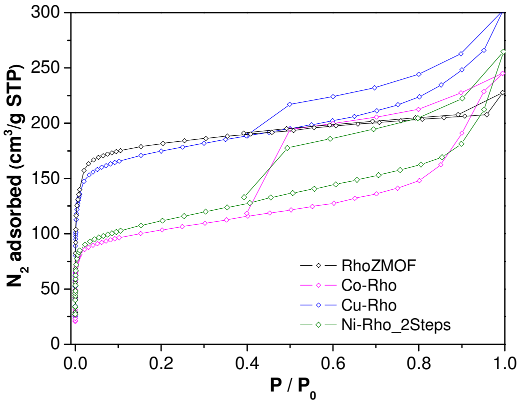

Fig. 8 N_2 adsorption-desorption isotherms at 77 K for RhoZMOF and Me-exchanged materials.

Table 1 Textural properties of Me-exchanged RhoZMOF materials obtained in the best conditions.

Material	t (h)	T (°C)	Me/In molar	% i.e.	S_{BET} (m^2/g)	V_p (cm^3/g)
RhoZMOF	-	-	-	0	705±25	0.34±0.1
Co-Rho	12	25	0.49±0.05	100±4	380±15	0.38±0.1
Cu-Rho	6	-20	0.15±0.02	30±1	670±20	0.39±0.1
Ni-Rho (2 steps)	4	25	0.09±0.02	18±1	405±15	0.29±0.1

Finally, N_2 adsorption-desorption at 77 K characterization test was carried out on order to estimate the textural properties for the best Me-exchanged RhoZMOF materials. Fig. 8 depicts type I isotherms regarding IUPAC classification[25] . For metal-exchanged materials a hysteresis loop is observed, indicating the appearance of an additional porosity possibly as a consequence of the formation of cavities in the meso, macro-pore range due to the partial rupture of the crystals during the ion-exchange treatment, as can be observed in the SEM images (Fig. 7). In addition, Table 1 shows textural properties of exchanged RhoZMOF materials, showing a reduction of the specific surface area (S_{BET}) and an increase of the pore volume (V_p) for these modified materials compared to the original RhoZMOF, probably due to the increase in the molecular weight and the smaller ion size of the compensating metal cations respect to HDMA$^+$ ones. The differences observed in textural properties among Me-exchanged materials are explained by the different ion-exchange extension achieved in the samples, since these three transition metal cations exhibit similar weight and size.

Conclusion

Co^{2+}, Ni^{2+} and Cu^{2+} inclusion in RhoZMOF structure have been achieved by carrying out an ion-exchange post-synthesis process. The best conditions for this modification treatment have been found for each transition metal ion, taking into account the different tendency in complexating with electron-donor moieties of the structure, i.e. compensating dimethyl ammonium cations. Particularly, complete exchange of HDMA$^+$ for Co^{2+} could be reached at room temperature after 12 h of contacting time of RhoZMOF crystals in the Co-rich aqueous solution. In the case of Cu^{2+}-exchange, a rapid transformation of RhoZMOF structure into a new crystalline Cu-rich phase was observed at room temperature, avoiding its appearance and preserving the desired structure when ion-exchange treatment is carry out at -20°C and 6 hours, reaching a partial ion-exchange degree of 30 %. For Ni^{2+} ion-exchange treatment, at 25 and 0°C, an amorphous Ni-rich organometallic phase over the crystals were detected by SEM analysis, presumably formed by the reaction of Ni^{2+} ions with $HDMA^+$ ions migrated to the surface of the crystals. The appearance of organometallic complex impurities can be successfully prevent when reducing the amount of $HDMA^+$ in the media by developing the ion-exchange process in two steps: $HDMA^+$ for Na^+ and Na^+ for Ni^{2+}. These results provide the opportunity of obtaining porous MOF materials containing open transition metal sites, accessible for redox catalysis and selective gas adsorption.

Acknowledgements

The authors wish to thank ''*Comunidad de Madrid*'' and Spanish Ministry of Science and Innovation for their financial support to the SOLGEMAC Project (S2009/ENE-1617) and CICYT Project (CTQ2012-38015). JAV acknowledges Spanish Science and Innovation Ministry for financial support (FPI BES-2010-032722).

References

1. O. Farha and J. Hupp, *Acc. Chem. Res.*, 2010, **43**, 1166.
2. S. Li and Q. Xu, *Energy Environ. Sci.*, 2013, **6**, 1656.
3. A. Morozan and F. Jaouen, *Energy Environ. Sci.*, 2012, **5**, 9269.
4. K. Park, Z. Ni, A. Côte, J. Choi, R. Huang, F. J. Uribe-Romo, H. K. Chae, M. O´Keefee and O. M. Yaghi, *Proc. Nation. Acad. Sci.*, 2006, **103**, 10186.
5. A. Phan, C. Doonan, F. Uribe-Romo, C. Knobler, M. O'Keeffe and O. Yaghi, *Acc. Chem. Res.*, 2010, **43**, 58.
6. Y. Liu, V. Kravtsov, R. Larsena and M. Eddaoudi, *Chem. Commun.*, 2006, 1488.
7. Y. Liu, V. Kravtsov and M. Eddaoudi, *Angew. Chem. Int. Ed.*, 2008, **47**, 8446.
8. F. Nouar, J. Eckert, J. Eubank, P. Forster and M. Eddaoudi, *J. Am. Chem. Soc.*,2009, **131**, 2864.
9. M. Alkordi, J. Brant, L. Wojtas, V. Kravtsov, A. Cairns and M. Eddaoudi, *J. Am. Chem. Soc.*,2009, **131**, 17753.
10. G. Calleja, J. Botas, M. Sánchez-Sánchez and M. Orcajo, *Int. J. Hydrogen Energy,* 2010, **35**, 9916.
11. C. Chen, J. Kim, D.-A. Yang and W.-S. Ahn, *Chem. Eng. Journal,* 2011, **168**, 1134.
12. G. Calleja, J. Botas, C. Martos, M. Orcajo and J. Villajos, *Adsorption Science & Technology,* 2012, **30**, 793.
13. .W. Zhou, H. Wu and T. Yildrin, *J. Am. Chem. Soc.,* 2008, **130**, 15268.
14. G. Kubas, *Chem. Rev.,* 2007, **107**, 4152.
15. D. Esquivel, A. Cruz-Cabeza, C. Jimenez-Sanchidrian and F. Romero-Salguero, *Microp. Mesop. Mater.,* 2013, **179**, 30.
16. G. Centi and S. Perathoner, *Catal. Today,*2010*,* **150**, 151-162.
17. C. Yuan, H. Wu, Y. Xie and X. Lou, *Angew. Chem. Int. Ed.,*2014, **53**, 1488.
18. Z. Chen, D. Higgins, A. Yu, L. Zhang and J. Zhang, *Energy Environ. Sci.,*2011, **4**, 3167.
19. A. Goursot, B. Coq and F. Fajula, *J. Catal.,* 2003, **216**, 324.
20. J. Zhou, Q. Xia, S. Shen, S. Kawi and K. Hidajat, *J. Catal.,* 2004, **225**, 128.
21. .W. Li, S. Yu, G. Meitzner and E. Iglesia, *J. Phys. Chem. B,* 2001, **105**, 1176.
22. H. Inokawa, S. Nishimoto, Y. Kameshima and M. Miyake, *Int. J. Hydrogen Energy,* 2010, **35**, 11719.
23. D. Halliche, O. Cherifi, Y. Taarit and A. Auroux, *Kinet. Catal.,* 2008, **49**, 667.
24. A. Stroppa, P. Jain, P. Barone, M. Marsman, J. Perez-Mato, A. Cheetham, H. Kroto and S. Picozzi, *Angew. Chem. Int. Ed.,* 2011, **50**, 5847.
25. K. Sing, D. Everett, R. Haul, L. Moscou, R. Pierrotti, J. Rouquérol and T. Siemieniewska, *Pure & Appl. Chem.,* 1985, **57**, 603.
26. M. Thommes, *Chemie Ingenieur Technik,* 2010, **82**, 1059.

Notes

[a] *Department of Chemical and Energy Technology, ESCET, Universidad Rey Juan Carlos, C/ Tulipán s/n, 28933 Móstoles, Madrid, Spain. Fax: 0034 914887068; Tel: 0034 914887006; E-mail: guillermo.calleja@urjc.es.*